ARTICLE OPEN

Check for updates

Sustained TNF signaling is required for the synaptic and anxiety-like behavioral response to acute stress

Gina M. Kemp[1], Haider F. Altimimi[1], Yoonmi Nho[1], Renu Heir[1], Adam Klyczek[1] and David Stellwagen[1]✉

Acute stress triggers plasticity of forebrain synapses as well as behavioral changes. Here we reveal that Tumor Necrosis Factor α (TNF) is a required downstream mediator of the stress response in mice, necessary for stress-induced synaptic potentiation in the ventral hippocampus and for an increase in anxiety-like behaviour. Acute stress is sufficient to activate microglia, triggering the long-term release of TNF. Critically, on-going TNF signaling specifically in the ventral hippocampus is necessary to sustain both the stress-induced synaptic and behavioral changes, as these could be reversed hours after induction by antagonizing TNF signaling. This demonstrates that TNF maintains the synaptic and behavioral stress response in vivo, making TNF a potential novel therapeutic target for stress disorders.

Molecular Psychiatry (2022) 27:4474–4484; https://doi.org/10.1038/s41380-022-01737-x

INTRODUCTION

Stress drives adaptive responses critical for an organism's physiological homeostasis and function. However, unregulated activation of the stress response results in significant problems; stress is a major contributing factor to the development of a number of psychiatric diseases including post-traumatic stress disorder and other anxiety disorders [1, 2]. There are long-standing observations of reciprocal interactions between stress and the immune system; stimulation of the immune system is a potent activator of the hypothalamic-pituitary-adrenal (HPA) axis, and the output of the HPA axis (corticosteroid (Cort)) can exacerbate inflammation in the brain under certain conditions or be an immune suppressant in other conditions [3–5]. Further, elevated pro-inflammatory cytokine levels are observed in patients with generalized anxiety disorder [6, 7] and even acute stressors can increase cytokines levels in humans [8, 9].

The role of cytokines in the stress response and development of anxiety is not clear. Immune signaling molecules appear to be involved in stress conditions, including chronic mild stress [10]; repeated social defeat [11]; stress-induced ischemia [12]; and HPA regulation [13]. Acute stress alone can induce peripheral cytokine production [14, 15], and cytokines are linked to the acute stress-induced development of anhedonia [16] and anxiety [17]. Tumor Necrosis Factor α (TNF) in particular may play a causal role in the development of anxiety-like behaviors, as blocking TNF signaling reduced the expression of anxiety-like behaviors induced by peripheral inflammation [18], chronic pain [19], obesity [20], or experimental autoimmune encephalomyelitis [21]. Moreover, elevating central TNF levels by direct intracerebroventricular injection increases anxiety-like behaviors in mice [21]. This suggests that it is possible that stress-induced anxiety is mediated by TNF.

A single bout of stress is reported to vary in its ability to stimulate TNF expression but generally observed to trigger an elevation [17, 22–26], similar to what is seen for chronic stress [10, 27]. In particular, acute exposure to a combination of restraint and water immersion will increase TNF levels in the hippocampus due to microglia activation [23]. The elevation of TNF in the hippocampus is intriguing as there is strong evidence to implicate the ventral hippocampus in the regulation of anxiety-like behaviour. Unlike the dorsal hippocampus, a key structure for spatial memory, the ventral hippocampus modulates emotional states [28, 29]. This is particularly true for anxiety, as lesioning the ventral hippocampus is anxiolytic [30, 31]. Anxiety-responsive cells are found in the ventral hippocampus, and optogenetic activation of the terminals of these cells in the lateral hypothalamic area increased avoidance and anxiety-like behaviour [32]. Critically, a variety of optogenetic and pharmacologic manipulation of the ventral hippocampus (and its inputs and outputs) directly alter anxiety-like behaviours [32–38]. The ventral hippocampus has also been shown to be involved in descending regulation of the HPA in response to acute stress [39].

However, whether the increase in hippocampal TNF is instructive to stress-related synaptic modulation and associated anxiety-like behaviors remains unexplored. In light of this, we investigated the mechanistic role for TNF, an inflammatory signaling molecule shown to play a role in the homeostasis of synaptic transmission [40], in the stress response. Here we demonstrate that acute stress induces TNF production within the ventral hippocampus. Further, sustained hippocampal TNF signaling is required to maintain the synaptic potentiation and the increase in anxiety-like behavior induced by acute stress.

MATERIALS AND METHODS

All experiments and procedures involving animal use were conducted in accordance with the guidelines of the Canadian Council on Animal Care and approved by the local Animal Care Committee of the Montreal General Hospital.

[1]Department of Neurology and Neurosurgery, Centre for Research in Neuroscience, Research Institute of the McGill University Health Center, Montréal, QC, Canada.
✉email: david.stellwagen@mcgill.ca

Received: 19 January 2022 Revised: 3 August 2022 Accepted: 9 August 2022
Published online: 14 September 2022

Animals

All experiments were done using adult C57BL/6 male mice, 8–16 week old for behavioral experiments and 8–12 week old for electrophysiology experiments. TNF homozygous knockout ($TNF^{-/-}$ mice), obtained from Jackson Labs, were bred in house, and compared with wild-type (WT) mice of the same background strain (C57BL/6J) also bred in house. The in-house WT and $TNF^{-/-}$ lines were periodically backcrossed. In some cases, WT C57BL/6 mice were obtained from Charles River, in which case they were housed in the animal facility for at least one week prior to experimentation. $TNFR1^{-/-}$ mice [41] were obtained from Jackson Labs and bred homozygously. Floxed TNF mice were obtained from S. Nedospasov [42] and crossed with GFAP-Cre mice [43] from NCI Mouse Repository (RRID: IMSR_NCIMR: 01XN3) or with Tg(Cx3cr1-cre)MW126Gsat mice [44] generated by N. Heintz (The Rockefeller University, GENSAT) and purchased from MMRRC (UC Davis; RRID: MMRRC_036395-UCD). GFAP or Cx3Cr1-Cre expressing mice were compared with GFAP or CX3CR1-Cre non-expressing littermates. Floxed TNF and GFAP-Cre mice were on a C57BL/6 background; Cx3Cr1-Cre mice were a mix of FVB/B6/129/Swiss/CD1 and backcrossed several generations with C57BL/6J. Animals were group housed (3–5 animals/cage, except following stress; see below) in standard controlled housing environment of 12 h light cycle, and food and water available ad libitum. Littermates were randomly assigned to the stress or non-stress groups.

Stress paradigms

Two stressors were used to verify the robustness of the phenotype: most animals were exposed to a forced swim of 20 min duration; the time of day in which the animals were exposed to stress was consistent throughout all experiments (10:00 AM–1:00 PM). Animals were placed in a 4 L glass beaker, filled to the 3 L mark with room temperature (23–25 °C) tap water. At completion, excess water was gently wiped off animals and they were housed individually thereafter, with food and water available ad libitum until experimentation. Other animals were exposed to immobilization stress through restraining them in 50 ml conical tubes (Sarstedt #62.547.205), perforated to allow for airflow. Tubes were then left undisturbed for 1.5 h at room temperature under regular room white fluorescent lighting conditions. Animals were again individually housed post-stress. There was no significant effect of short-term single housing on TNF protein levels in the vHPC (Supplementary Fig. 9A) or on anxiety-like behavior (Supplementary Fig. 9B), so single-housing as described does not constitute a significant stressor on its own.

Cannula implantation and local injections

Bilateral cannulation was performed on 8-week-old mice with a recovering period of three-four weeks to allow inflammation to subside. Animals were administrated an analgesic (Carprofen; SC, 20 mg/kg) 2 h before the surgery then anaesthesia was induced at 3% isoflurane and maintained at 2% throughout the surgery. Animals were injected with 1 ml of warm saline at the beginning and the end of the surgery to prevent dehydration and were kept on an active heating pad to reduce anaesthesia-induced hypothermia (PhysioSuite, Kent Scientific). Eye lubricant was repeatedly applied throughout the surgery to prevent eye damage. Cannulae were stereotaxically implanted into the ventral hippocampi at coordinates (relative to Bregma) of AP −3.31 mm, ML ± 3.47 mm, DV −4.6 mm; and secured with dental cement.

The skin was closed with braided silk sutures (Medtronic, KENS1173) and cannula caps were placed to prevent clogging. Animals were allowed to recover in heated cages, and administrated Carprofen (20 mg/kg/day) for three days. Post-op animals were group-housed for 3–4 weeks, and then exposed to 1.5 h restraint stress and single housed from then on. DN-TNF or saline was administrated 5 hr post-stress, using an injection cannula attached to a Hamilton syringe and a micropump at a rate of 0.2 µl/min to inject 0.625 µl in each hemisphere. The injection cannula was then kept in place for 1–2 min before removal to prevent backflow. The injection apparatus was checked before and after each injection to ensure proper flow. Animals were returned to their cages and then behaviorally tested 48 h post-stress. Injection sites were verified by histology to be in the ventral hippocampus for all animals; a representative injection site is show in Supplementary Fig. 10.

Electrophysiology

Synaptic glutamatergic currents were measured from animals that were housed under control conditions or at 2–24 h post-stress (AMPA/NMDA ratios) or 24 h post-stress (I/O curves). A few cells for I/O curves were sampled at 2 h post-stress, but since there was no difference in the potentiation of AMPA/NMDA ratios or AMPAR-mediated currents observed 2 h and 24 h post-stress, data from these time points were pooled. Animals were anesthetized by isoflurane inhalation, and rapidly perfused through the left cardiac ventricle with ice-cold solution (composition in mM: glycerol 222, D-glucose 11, $NaHCO_3$ 26, KCl 2.5, NaH_2PO4 1.25, $MgCl_2$ 3.5, $MgSO_4$ 1, $CaCl_2$ 0.25, Na pyruvate 1.5, Na ascorbate 0.4) pre-saturated with 95% O_2/5% CO_2. The brain was then removed and horizontal slices of 300–400 µm, containing the ventral hippocampus, were cut on a vibrating slicer (Leica VT1200S) in the same solution used for perfusion, followed by recovery of slices at 32 ± 2 °C for 30–45 min in solution of composition (in mM): NaCl 118, D-glucose 11, $NaHCO_3$ 26, KCl 2.5, HEPES 15, NaH_2PO_4 1.25, $MgSO_4$ 1, $CaCl_2$ 2, myo-inositol 3, Na ascorbate 0.4, saturated with 95% O_2/5% CO_2; slices were maintained at room temperature thereafter, and were only used for experiments after a minimum of 1 h incubation post-slicing.

Immediately prior to placing brain slices in a perfusion chamber on the stage of an upright Olympus microscope (BX51WI) equipped with IR-DIC optics, a cut was made between CA3 and CA1. Using Clampex to run Multiclamp 700 with Digidata 1440 (Molecular Devices), voltage-clamp recordings at holding potential of −70 mV (unless otherwise specified) were acquired, at 10 kHz sampling with 2 kHz low-pass filtering, from visually identified CA1 pyramidal cells using borosilicate glass pipette electrodes, pulled to produce a resistance of 2–5 MΩ when filled with internal solution of composition (in mM): $CsMeSO_4$ 125, CsCl 10, HEPES 15, MgATP 4, Na_3GTP 0.4, Na_2-phosphocreatine 5, Trisphosphocreatine 5, EGTA 0.6, $CaCl_2$ 0.05, pH adjusted to 7.2 with CsOH. Bath solution containing (in mM): NaCl 110, D-glucose 11, $NaHCO_3$ 26, KCl 2.5, HEPES 15, NaH_2PO_4 1.25, $MgSO_4$ 1, $MgCl_2$ 3, $CaCl_2$ 4, myo-inositol 3, and saturated with 95% O_2/5% CO_2 was perfused at a rate of 4–8 mL/min, and maintained at 30 ± 2 °C. In all experiments, the bath solution was supplemented with 100 µM picrotoxin to block $GABA_A$R-mediated currents; 50 µM D-AP5 was added to isolate AMPAR currents, while 15 µM NBQX was added and the holding potential adjusted to +40 mV to isolate NMDAR currents. To evoke synaptic responses, a stimulus isolator (ISO-FLEX, A.M.P.I.) was used to deliver constant current stimuli (0.1 ms pulse duration) to stratum radiatum, using either a chlorided silver wire housed in a glass pipette filled with bath solution, or, in the case of obtaining input-output relationships, matrix electrodes fabricated by FHC (MX21AES(DH1)). Care was taken in the case of obtaining input-output relationships to systematically place the stimulating electrode within ~20 µm of the cell being recorded, and control condition recordings were consistently interleaved throughout the period of experimentation. Stimuli were delivered at intervals of 5–15 s, and 6–30 sweeps were averaged for any given stimulus level (using Clampfit 10). AMPA/NMDA ratios were obtained by dividing the peak of the evoked current generated while the cell is held at −70 mV by the mean level of the current 50 ms from the onset of stimulus while the cell is held at +40 mV. Alternatively, a subset of cells was perfused with 50 µM D-AP5 while held at +40 mV, and the resultant isolated AMPAR current obtained following D-AP5 perfusion was subtracted from the compound current prior to perfusion with D-AP5 to obtain the NMDAR component of the evoked response, in which case the peak of the AMPAR current was divided by the peak of the resultant NMDAR current.

Drug treatments

For experiments involving corticosterone treatment, corticosterone stock prepared in DMSO was diluted to 100 nM and applied to brain slices in the solution used for recovery from vibratome slicing, for 20 min at 30 ± 2 °C, with constant aeration with 95% O_2/5% CO_2. Slices were then washed with corticosterone-free solution, and then incubated in slice recovery solution. Voltage-clamp recordings were obtained between 2–3 h following corticosterone treatment. Controls were likewise treated, but with vehicle (0.01% v/v DMSO). Metyrapone was obtained from Tocris Bioscience #3292/50 and reconstituted to 23 mg/ml with DMSO and administrated intraperitoneally at a final doze of 50 mg/kg. TNF dominant-negative inhibitor XPro1595 (DN-TNF; Xencor, Inc.) was diluted in sterile 0.9% w/v NaCl to 2 mg/mL (intraperitoneal injection) or 5 mg/ml (direct injection into the hippocampi) and administered at a dose of 20 mg/kg. Controls were administered equivalent volumes of DMSO or sterile saline 0.9% w/v NaCl, respectively.

Cort ELISA

Stress-induced serum corticosterone measures were obtained 15 min following completion of forced swim protocol. Animals were anesthetized

by isoflurane inhalation, decapitated, and trunk blood collected in polypropylene centrifuge tubes. Samples were stored at room temperature for 1.5 h to allow for clot formation, followed by centrifugation (300 x **g**) to collect supernatant for storage at −80 °C until assayed. An ELISA kit from Cayman for corticosterone was used according to the suppliers' instructions. Samples were diluted 100-fold prior to measurement.

TNF ELISA

Bilateral ventral hippocampal tissue was collected from stressed animals (24 h post forced swim stress) and their age-matched unstressed controls. They were anesthetized by isoflurane inhalation and decapitated for a rapid removal of the brain and gross dissection of the ventral hippocampi (<1 min). Tissue was then snap-frozen in liquid nitrogen. Tissue was then immediately homogenized using a handheld homogenizer for 5 s on ice in 400 µl of sterile PBS buffer containing a 1x protease inhibitor cocktail from Bioshop (PIC002.1). Samples were then centrifuged at 11,000 rpm for 20 min at 4 °C and the supernatants collected. TNF protein levels were measured according to the suppliers' instructions of mouse TNF ELISA kit (eBioscience, Mouse TNF alpha ELISA Ready-SET-Go! Kit #88–7324). For standardization across samples, all TNF concentrations were divided by their corresponding crude-protein input concentrations as measured following the instructions of the bicinchoninic acid assay (BCA) kit from Thermo Fisher Scientific (#23227).

c-Fos Immunohistochemistry

One hour following stress, animals were anesthetized by isoflurane inhalation, followed by transcardial perfusion with 4% w/v formaldehyde in PBS. The brain was then dissected and immersed in 4% w/v formaldehyde for 24 h at 4 °C, then transferred to 30% w/v sucrose solution. The brains were subsequently mounted in Optimal Cutting Temperature (OCT) medium to cut 30 µm slices using cryostat microtome. Slices were incubated in a blocking solution, composition: 2% v/v normal goat serum and 1% v/v affinipure donkey anti-mouse IgG (Jackson Immunoresearch) in PBS for 4 h at room temperature. Slices were subsequently incubated with primary antibodies: anti-c-Fos at 1:100 dilution (Santa Cruz Biotechnology, catalogue sc-52) and anti-NeuN at 1:200 (Millipore, catalogue MAB377) in blocking solution overnight at 4 °C. Slices were then washed twice (15 min each wash) with PBS + 0.05% Tween 20 (PBST), and once in PBS for 15 min, and incubated with secondary antibodies: Alexa568-conjugated anti-rabbit IgG at 1:300 dilution and Alexa488-conjugated anti-mouse IgG at 1:400 dilution in blocking buffer for 2 h at room temperature. Slices were then washed twice (15 min each wash) with PBS + 0.05% Tween 20 (PBST), and once in PBS for 15 min, followed by mounting in Fluoromount-G medium (Southern Biotech). Images were acquired with an Olympus Fluoview FV1000 confocal microscope using 20X objective. 25–30 optical sections at 1 µm optical sectioning were collected, and Z-projected into a single image. Multiple images of region CA1 and DG were collected for each animal, and the number of c-Fos immunoreactive cells were manually counted, and averaged for all slices to give one mean value for each animal. For clarity, the c-Fos-labeled sections used as example images shown were background subtracted and despeckled using ImageJ (NIH), followed by conversion to binary format and dilation, and then overlaid with corresponding NeuN-labeled sections.

IBA1 Immunohistochemistry and microglial analysis

Animals were perfused 4 h post-restraint stress with 4% PFA in PBS, and whole brains post-fixed overnight (~16 h) before being cryoprotected in 30% sucrose in PBS for 4 h. Coronal 25 µm sections containing the ventral hippocampus were cut on a cryostat, mounted on charged slides (Fisher Scientific, catalogue 12–550–15) and dried in a desiccating chamber at room temperature for 2 h. Sections were then washed 3x with PBS at room temperature (10 min) followed by 1 h permeabilization using 2% triton X-100 in PBS. Sections were blocked for 2 h with 10% normal goat serum, 2% BSA, and 0.3% Triton X-100, and then incubated overnight at 4 °C with IBA1 polyclonal rabbit antibody (FUJIFILM Wako Chemicals, catalogue 019-19741; 1:500) in blocking buffer. Sections were then washed as before and incubated in goat anti-rabbit secondary antibody (Thermofisher, A21244), washed 4x, and nuclei counterstained with 1:10,000 of Hoechst 33342 (Thermofisher H1399) before mounting with Fluoromount-G (Thermofisher, 00-4958-02). Stacked Images were acquired using FV1000 Olympus confocal microscope using 20x objectives of the vCA1 region, with multiple images per animal. Images were then analyzed for signal intensity, cell count, and morphology semi-automatically using ImageJ (NIH) and its associated FracLac package (Karperien). Average values were calculated per field, with the researcher blinded during both acquisition and analysis. The images were converted to grayscale, unsharpened, despeckled, thresholded automatically, and converted to a binary mask. The "analyze particles" function was then applied with size thresholding of 50 pixels on the lower limit. The obtained ROIs were then checked manually for accuracy then were overlayed over the original image to obtain the reported outputs. Microglia morphology was evaluated using a hull and circle analysis, by fitting each microglia with an encompassing oval/circle and a convex hull. Morphology was then assessed by measuring the polarity of these shapes as a ratio of the major and minor axes and hull circularity as the hull area over the perimeter, with a loss of polarity representing an increase in activation.

Behavior

All behaviour experiments were verified using multiple cohorts and replicated across different time intervals. Animals were tested 24–48 h following stress, and experiments were conducted between 10:00 AM and 5:00 PM (anxiety) or 4:00–7:00 PM (locomotion). Anxiety-related behavior was assessed using the Light-Dark box, which consisted of an uncovered compartment (light compartment) made of clear plexiglass, measuring 29 cm length × 20.4 cm width × 22 cm height, connected via a small box-floor level opening to a black, lid-covered compartment (dark compartment) measuring 15.5 cm length × 20.4 cm width × 22 cm height. The animal was placed in the dark compartment with the animal allowed to freely explore both compartments for a period of 10 min while video recording from directly above. The test was conducted under normal room white fluorescent lighting. The total time spent in the light compartment was scored semi-automatically using Ethovision XT 8.5 (Noldus). Anxiety-like behavior was also assessed in the Open Field Test using a 60 × 60 cm clear plexiglass box under normal room lighting conditions. The time spent in the center (out of the total testing time of 10 min) was quantified automatically using the pre-existing template in Ethovision. For assessing locomotion, proxied by the total distance travelled during a period of 20 min, animals were placed individually in 30 × 30 cm plexiglass boxes recorded from above under low-intensity red light conditions. The total distance travelled during the 20 min period was then recorded automatically using Ethovision. As all behavior was analyzed by the computer, experimenters were not blind to treatments.

Statistical analysis

All data are presented as means ± SEM. In electrophysiology data, n represents the number of cells, while N represents the number of animals; no more than three cells were recorded from any given animal, with all experimental groups being represented by at least three animals. Statistical analyses were done using Graphpad Prism 9. Data was analyzed using one or two-way ANOVAs, followed by Tukey post-hoc tests, or by Student's unpaired two-tailed t-tests. For Fig. 3A, the data was not normally distributed, so we used a Kruskal-Wallis One Way ANOVA on Ranks followed by Dunn's method of comparison with control. Other comparison groups had similar variances; sample sizes were not estimated in advance.

RESULTS

We used an acute stressor to study the role of TNF on subsequent stress-induced synaptic and behavioral changes (Fig. 1A). Exposure of adult male mice to 20 min of forced swimming (at 23–25 °C) was sufficient to increase anxiety-like behaviour 24 h later as measured by both the light-dark box and open field test (Fig. 1B). This effect was not stressor dependent, as 1.5 h of restraint stress caused a similar increase in anxiety-like behaviour, measured 24 h later, using the light-dark box (Fig. 1C). The canonical stress pathway is necessary for this stress-induced increase in anxiety-like behaviour: inhibiting Cort production, the principal terminal output of the HPA axis, via metyrapone administration (IP; 50 mg/kg; 1 h pre-stress) blocked the behavioral changes seen in the WT animals (Fig. 1D).

Several studies have reported that acute stress induces TNF expression in the forebrain for up to seven hours [17, 23–25], but the role for this persistent elevation remains unclear. In response

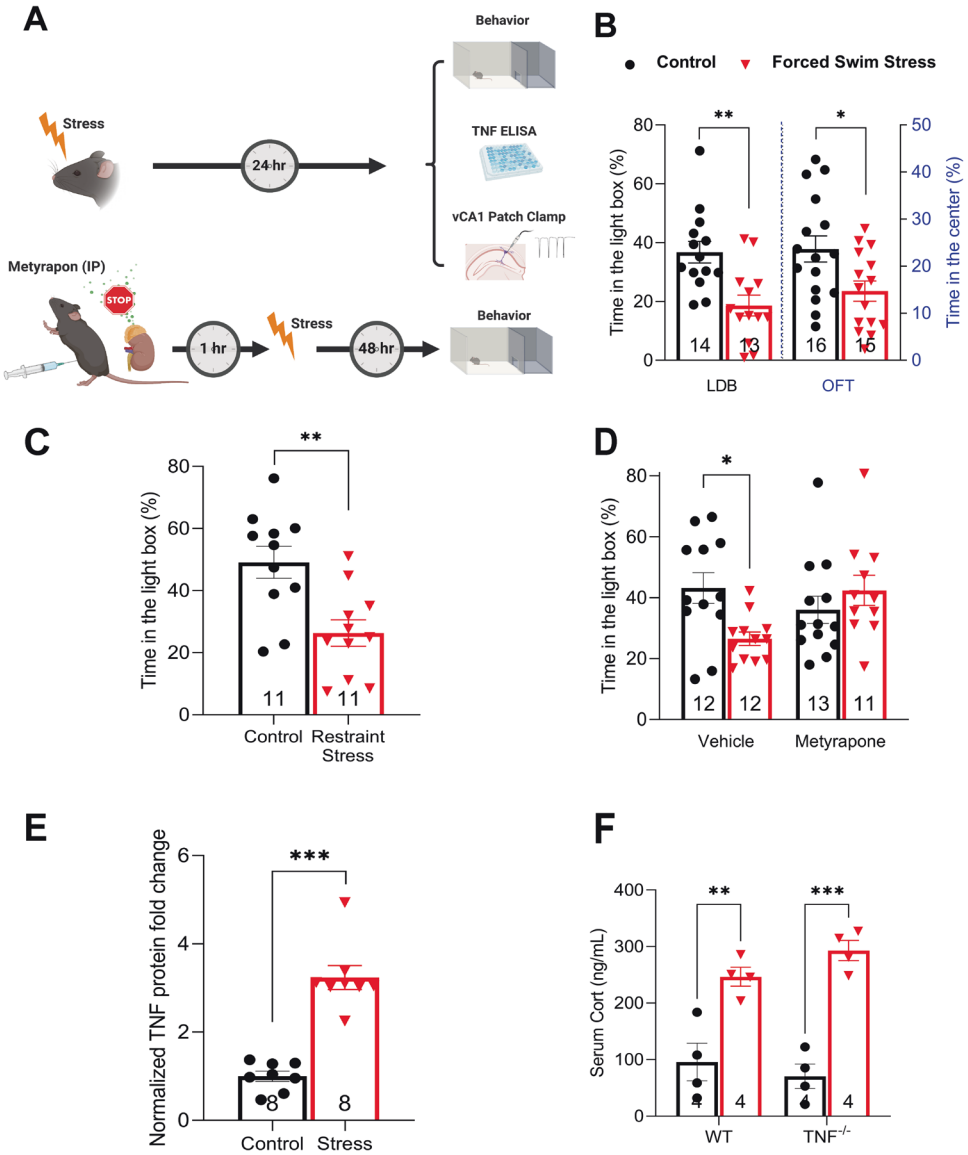

Fig. 1 Molecular and behavioral characterization of acutely stressed mice. A. A general schematic of the conducted experiments. For most experiments, mice were subjected to a single bout of acute stress and tested 24 h later. Some mice were given metyrapone 1 h prior to stress and then tested 48 h later. **B** Animals subjected to forced swim stress display anxiety-like behavior, as measured in the LDB (two-tailed student *t*-test $p = 0.0015$) and the OFT (two-tailed student *t*-test $p = 0.0171$). **C** The induction of anxiety-like behavior in males is also observed in response to RS paradigm (two-tailed student *t*-test, $p = 0.0028$). **D** Blocking CORT synthesis through administering metyrapone (IP; 40 mg/kg; 1 h pre-stress) inhibits stress-induced anxiety-like behavior (significant interaction of stress × drug; two-way ANOVA $F(1, 44) = 7.051$, $p = 0.0110$; Tukey's post hoc analysis of control versus stress within vehicle $p = 0.0444$, within metyrapone $p = 0.7281$). **E** Acute swim stress induces significant induction of TNF protein in the vHPC measured 24 h post-stress ($p < 0.0001$). **F** Swim stress induces serum CORT levels independent of TNF signaling (ANOVA $F(1, 12) = 63.79$, $p < 0.0001$; Tukey's post hoc analysis of control versus stress within WT animals $p = 0.0031$, within $TNF^{-/-}$ animals $p = 0.0001$). $^{*}p < 0.05$, $^{**}p < 0.01$, $^{***}p < 0.001$. Data are presented as mean ± SEM. TNF tumor necrosis factor, CORT corticosterone, LDB light-dark box. OFT open field test. Sample sizes are indicated on the figures.

to forced swim stress, we observed a robust elevation in TNF protein in the ventral hippocampus at 24 h post-stress (Fig. 1E).

To investigate the role of elevated TNF in the initiation or expression of the stress response, we began by comparing circulating Cort levels between wildtype (WT) and TNF deficient $TNF^{-/-}$ mice, both under basal conditions as well as shortly after exposure to acute swim stress. We found no significant differences under either condition (Fig. 1F), demonstrating that TNF is not involved in regulating circulating Cort levels basally nor its release following stress. Stress is also known to be a potent activator of immediate early gene expression in the hippocampus [45]. Synaptic output from ventral hippocampus is strongly linked to the expression of anxiety-related behaviours [32, 38] and this region is involved in descending regulation of the HPA in response to acute stress [39]. Therefore, we tested whether $TNF^{-/-}$ animals have a normal c-Fos response to stress in the ventral hippocampus. We observed that the stress-induced increase in c-Fos expression was comparable between $TNF^{-/-}$ and WT animals (Supplementary Fig. 1). As a whole, these data suggest Cort regulation is independent of TNF, and thus TNF would more likely be a downstream mediator of the stress response.

To test the role of TNF in the expression of stress-induced behavioral change, we next examined the difference in stress-

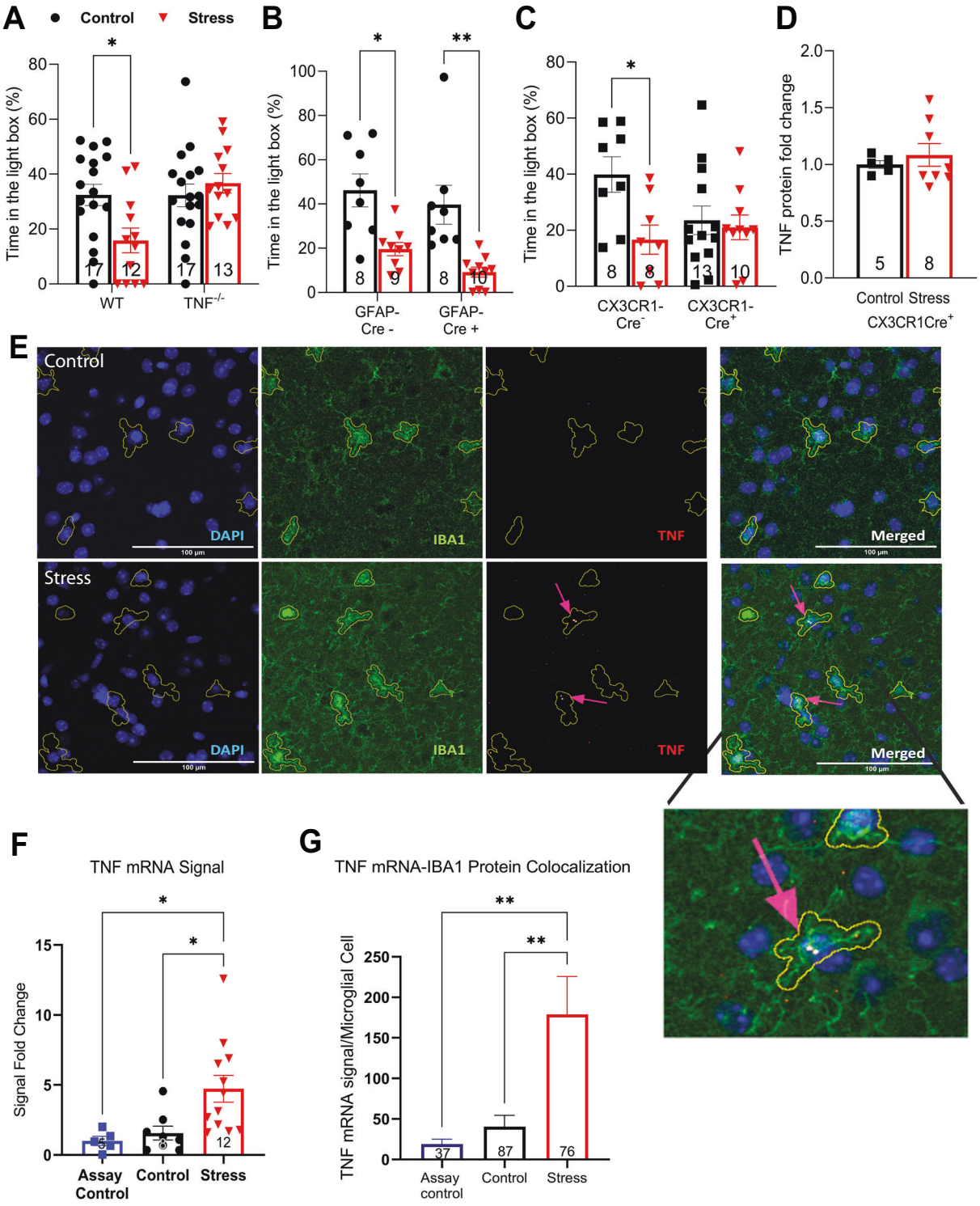

induced changes in anxiety-like behaviour between WT and *TNF*$^{-/-}$ mice. Using the light-dark box, *TNF*$^{-/-}$ mice spent an equivalent amount of time in the light compartment as their WT counterparts under control conditions but importantly did not show any decrease in this measure following stress (Fig. 2A). Mice lacking TNF also did not have the normal anxiety-induced increase in latency to enter the light compartment and decrease in transitions between the compartments (Supplementary Fig. 2). Similarly, mice lacking the principal receptor for TNF (*TNFR1*$^{-/-}$) also had normal baseline behaviour but no stress-induced elevation in anxiety-like behaviour (Supplementary Fig. 3).

The stress-induced elevation in TNF appears to be microglial in origin. Mice with a specific deletion of TNF from astrocytes (using GFAP-Cre combined with floxed TNF alleles) have an equivalent increase in anxiety-like behaviour following stress as their Cre negative littermates (Fig. 2B). However, conditional deletion of TNF from microglia using CX3CR1-Cre prevented the increase in anxiety-like behavior in stressed CX3CR1-Cre positive mice relative

Fig. 2 Microglial TNF signaling is important for the induction of stress-induced anxiety-like behavior. A. Mice that lack global TNF production do not show induction in anxiety-like behavior. (two-way ANOVA genotype x stress interaction $F(1, 55) = 6.536$, $p = 0.0134$; Tukey's *post hoc* analysis of control versus stress within WT $p = 0.0324$, $TNF^{-/-}$ $p = 0.8689$). **B** Stress induces anxiety-like behavior in GFAP-Cre positive animals compared to their unstressed GFAP-Cre positive counterparts, similar to the phenotype in WT animals (24 h; two-way ANOVA main effect of stress $F(1, 31) = 25.53$, $p < 0.0001$; Tukey's *post hoc* analysis: Cre negative control versus stress $p = 0.0127$, Cre positive control versus stress $p = 0.0028$). **C** Stressed CX3CR1-Cre positive animals lack a stress-induced increase in anxiety-like behavior compared to their unstressed counterparts. Control CX3CR1-Cre negative animals do have a stressed-induced increase in anxiety-like behaviour, which is comparable to WT (24 h; two-way ANOVA main effect of stress $F(1, 35)$, $p = 0.0227$; main effect of genotype $F(1, 35) = 1.222$, $p = 0.2765$; interaction of stress x genotype $F(1, 35) = 3.679$, $p = 0.0633$). Tukey's *post hoc* reveals that for Cre negative animals, control versus stress $p = 0.0384$ while for Cre positive, control versus stress $P = 0.9836$. **D** Microglial-TNF-lacking animals lack stress-induction of TNF in the vHPC compared to their controls (two-tailed student *t*-test, $p = 0.5355$). **E** Sample images demonstrating the results of RNAscope in situ hybridization combined with IBA1 immunohistochemistry staining in the vCA1-SR, using a bacterial probe and TNF mRNA probes in unstressed controls and stressed animals. The results are quantified in **F**, **G**. **F** Stress induces TNF mRNA in the SR of the vHPC (4 h post-stress; one-way ANOVA, main effect $F(2,22)$, $p = 0.0096$; Tukey's *post hoc* analysis of control versus stress $p = 0.0288$, stress versus nonspecific signal $p = 0.0271$, control versus nonspecific signal $p = 0.9182$, Sample size *n* (number of animals N) for assay control = 5 (3), for unstressed controls = 8 (4), for stressed animals = 12 (6)). **G** Quantification of the overlap in in situ hybridization signal and microglial cells in all three conditions. (4 h post-stress; one-way ANOVA main effect $F(2, 197) = 7.144$, $p = 0.001$; Tukey's *post-hoc* analysis of control versus stress $p = 0.0029$, control versus nonspecific signal $p = 0.9108$, stress versus nonspecific signal $p = 0.0082$, number of detected microglia n' (number of sections *n*–number of animals N) for assay control = 37 (3-2), for unstressed controls = 87 (6-3), for stressed animals = 76 (5-3)). $*p < 0.05$, $**p < 0.01$, $***p < 0.001$. Data are presented as mean ± SEM. TNF tumor necrosis factor; vHPC ventral hippocampus. Sample sizes are indicated on the figures.

to their unstressed CX3CR1-Cre expressing littermates, although there was a baseline behavioural shift in these animals (Fig. 2C). Control littermates who were negative for Cre-expression had normal stress-induced increases in anxiety-like behaviour (Fig. 2C). These data were corroborated by the lack of stress-induced elevation of hippocampal TNF in animals lacking microglial TNF (Fig. 2D). Consistent with an increase in microglia activation, we also observed a stress-induced increase in IBA1 immunostaining in the ventral hippocampus and a shift to a less polarized microglial morphology (Supplementary Fig. 4). We further used RNAscope to label TNF mRNA in sections from the same animals. Analysis of the stratum radiatum of the ventral hippocampus revealed a stress-induced increase in TNF mRNA labeling (Fig. 2E–F) as well as an increase in TNF mRNA associated with microglia (Fig. 2G). This is consistent with the stress-induced activation of microglia observed previously by others [15, 46].

Acute stressors, including forced swim and restraint, have been shown to modify basal glutamatergic transmission in a Cort-dependent manner at several structures, including cortex, the hippocampus, and the VTA [47–50]. We focused on the synapses within the ventral hippocampus, due to the strong linkage of this region with anxiety-like behaviors. We assessed glutamatergic transmission at Schaffer Collateral (SC) to CA1 synapses in the ventral hippocampus. Acute swim stress resulted in an increase in the AMPA/NMDA ratio at the SC synapses on CA1 pyramidal cells, relative to control mice left in their home cages. This potentiation was evident within 2 h and was sustained for at least 24 h (Fig. 3A and Supplementary Fig. 5A). Acute stress has been demonstrated to induce plasticity of AMPA receptor (AMPAR) currents, NMDA receptor (NMDAR) currents, or both, depending on brain structure examined [47, 49, 51]. Given this, we pharmacologically isolated AMPAR or NMDAR currents and assessed stimulus input-current output (I-O) relationships 24 h following stress. We found that AMPAR-mediated transmission was significantly potentiated (Fig. 3B) while there was no significant change in NMDAR-mediated transmission (Fig. 3C). Some studies have demonstrated a pre-synaptic locus of expression of enhanced glutamatergic transmission shortly following acute stress [52, 53], but we observed no changes in pre-synaptic glutamate release, as measured by the coefficient of variability (CV) and paired-pulse ratio (PPR) (Supplementary Fig. 5B, C). Since acute stress or glucocorticoid administration have also been shown to alter expression of some intrinsic voltage-gated currents and ion channel subunits [54–56], we also compared basic cellular electrophysiological properties of CA1 pyramidal cells - resting membrane potential, membrane resistance, and membrane capacitance - between stress and control groups and found them unchanged (Supplementary Fig. 5D–F). This suggests that the observed potentiation of glutamatergic transmission in ventral hippocampal SC to CA1 synapses is principally due to post-synaptic AMPAR trafficking, as has been shown for prefrontal cortex pyramidal cells [48].

We then tested the TNF dependence of this increase in AMPAR-mediated currents. We first determined that basal AMPAR-mediated transmission in the ventral hippocampus was not significantly different between WT and $TNF^{-/-}$ animals (Supplementary Fig. 6A). However, $TNF^{-/-}$ animals did not show potentiation of AMPAR currents after being exposed to acute stress in vivo; instead AMPAR currents tended to be depressed following stress (Fig. 3D). Stress-induced Cort release has generally been assumed to directly drive associated in vivo synaptic changes, in part because ex vivo [57] or in vitro [48, 58] application of Cort can potentiate synapses. We, therefore, tested the ex vivo Cort response of WT and $TNF^{-/-}$ hippocampal slices. In marked contrast to the in vivo results, TNF was dispensable for the ex vivo Cort-induced potentiation of AMPAR current at CA1 synapses in the ventral hippocampus (Supplementary Fig. 7). This suggests that ex vivo application of Cort does not replicate the in vivo mechanism, where TNF signaling is required.

To address potential off-target effects stemming from our use of germline $TNF^{-/-}$ animals, we turned to a pharmacological strategy using the brain-permeant reagent XPro1595, a well-established dominant negative version of TNF (DN-TNF) that antagonizes TNF signaling in a temporally constrained manner [59], by integrating into existent TNF trimers and preventing receptor binding. Pre-administration of DN-TNF (IP; 20 mg/kg) 18 h prior to exposing WT mice to stress (Fig. 4A) completely blocked the subsequent stress-induced potentiation of AMPAR synaptic currents (Fig. 4B, C). This was specific to the potentiated synapses since DN-TNF administration under control conditions did not alter basal synaptic transmission (Supplementary Fig. 6B). These data indicate that TNF is required during the stress response for the subsequent synaptic changes. As in vivo TNF-mediated synaptic changes are not typically long-lasting [60, 61], this suggests that persistent TNF signalling might be necessary to maintain the potentiation. To address this, we first tested whether the stress-induced synaptic plasticity could be reversed following the induction and expression of the potentiation, which occurs within 2 h (see Fig. 3A). Indeed, we found that administering DN-TNF to animals 5–24 h after swim stress (Fig. 4D) was sufficient to reverse the stress-induced synaptic potentiation at 48 h post-stress (Fig. 4E, F).

We then proceeded to test the behavioral consequences of this protocol. As with the synaptic potentiation, administration of DN-TNF 5 h after swim stress completely abrogated the anxiety-like phenotype seen in the saline treated cohort (Fig. 4G). These results were replicable using restraint stress, as administering DN-TNF 5 h

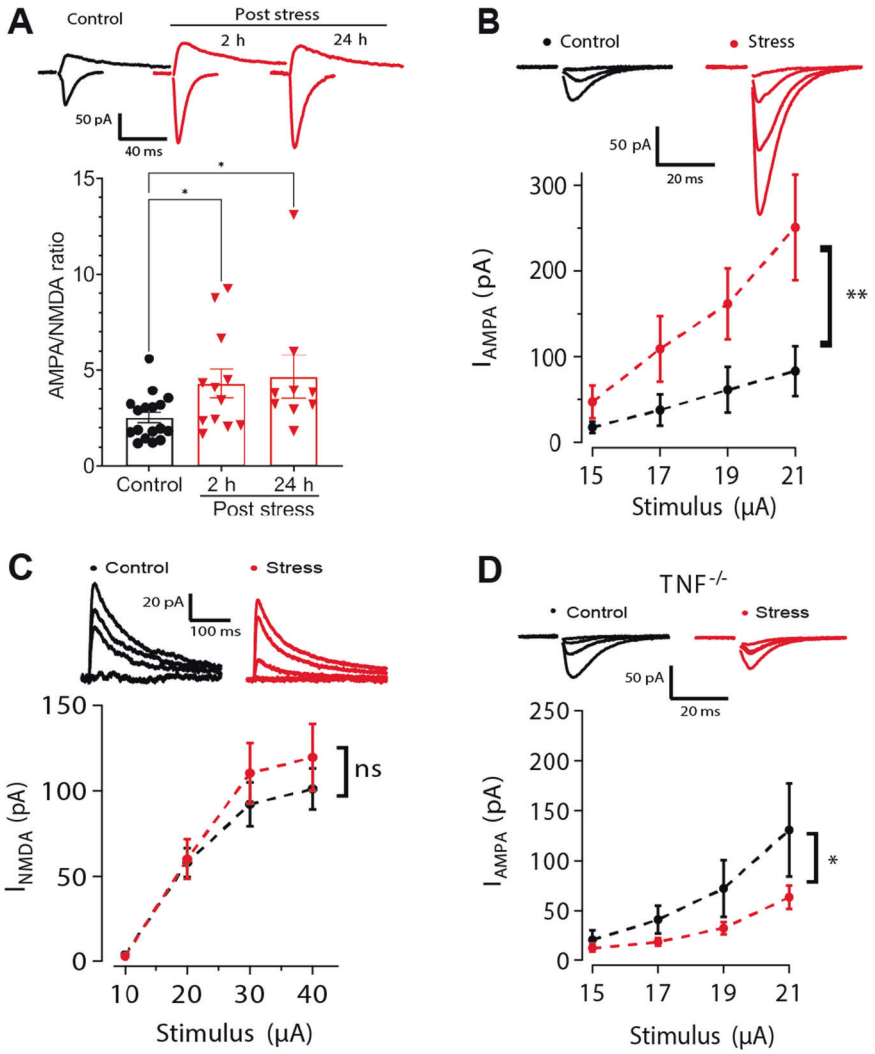

Fig. 3 AMPAR-mediated currents at the Schaffer collateral synapses in vCA1 are potentiated in WT animals and not in *TNF*$^{-/-}$ mice. A. Acute swim stress increases the AMPA/NMDA current ratio at Schaffer collateral synapses in the vCA1 at 2 and 24 h post-stress, as seen in sample traces and group data (Kruskal Wallis H(2) = 8.068, $p = 0.0177$; Control: $n = 17$, $N = 11$; 2 h post-stress: $n = 13$, $N = 8$; 24 h post-stress: $n = 9$, $N = 5$). **B** Stress potentiates the AMPA receptor (AMPAR) input-output relationship in the ventral Schaffer collaterals (24 h post-stress; two-way ANOVA of the main effect of stress F (1,40) = 11.439, $p = 0.0016$; control: $n = 5$, $N = 4$, stress: $n = 7$, $N = 3$). **C** There is no significant stress-induced potentiation of the NMDA receptor (NMDAR) mediated input-output curve in the ventral Schaffer collaterals (24 h post-stress; two-way ANOVA of the main effect of stress F (1,52) = 1 .0999, $p = 0.2991$; control: $n = 7$, $N = 4$, stress: $n = 8$, $N = 4$). **D** TNF lacking animals ($TNF^{-/-}$) do not exhibit potentiation in the AMPAR currents in the ventral hippocampus in response to stress-exposure (24 h post-stress; two-way ANOVA of the main effect of stress F (1, 44) = 6.315, $p = 0.0157$; control: $n = 6$, $N = 3$, stress: $n = 7$, $N = 4$). *$p < 0.05$, **$p < 0.01$, ***$p < 0.001$. Data are presented as mean ± SEM. Sample sizes are indicated on the bar figure or in the caption.

after this stressor also blocked the stress-induced increase in anxiety-like behavior (Fig. 4H). This was dependent on TNF signaling within the ventral hippocampus, as local injection of DN-TNF bilaterally into the ventral hippocampus was sufficient to block the expression of stress-induced anxiety-like behavior relative to littermates injected with saline (Fig. 4I). Neither stress, drug, nor mode of administration impacted the locomotor behaviour of the animals (Supplementary Fig. 8). We, therefore, conclude that acute stress induces on-going TNF signalling within the ventral hippocampus that is required to maintain the synaptic and behavioral outcomes of the stressor, in particular anxiety-like behaviours.

DISCUSSION

This TNF-mediated potentiation correlates with the stress-induced increase in anxiety-like behavior, and blocking TNF-signaling even hours after the stressor reverses both the synaptic potentiation and anxiety-like behavior.

Our results here reveal a novel property of the in vivo stress response, dissecting the response into at least two distinct phases: an induction phase and a maintenance phase. Importantly, we did not observe any gross abnormalities in the neuroendocrine axis of TNF deficient animals, nor in the stress-induced expression of the immediate early gene *c-Fos*, again highlighting that the deficit these animals exhibit with respect to the stress response appears limited to a lack of expression of a specific form of synaptic plasticity.

The induction phase is likely Cort-dependent, as blocking Cort production with metyrapone prevented the stress-induced anxiety. Previous results have also implicated Cort in the synaptic potentiation [2, 47, 49, 62]. However, the majority of work suggesting that Cort directly drives the potentiation comes from in vitro application of Cort [48, 57, 58]. While we can replicate the

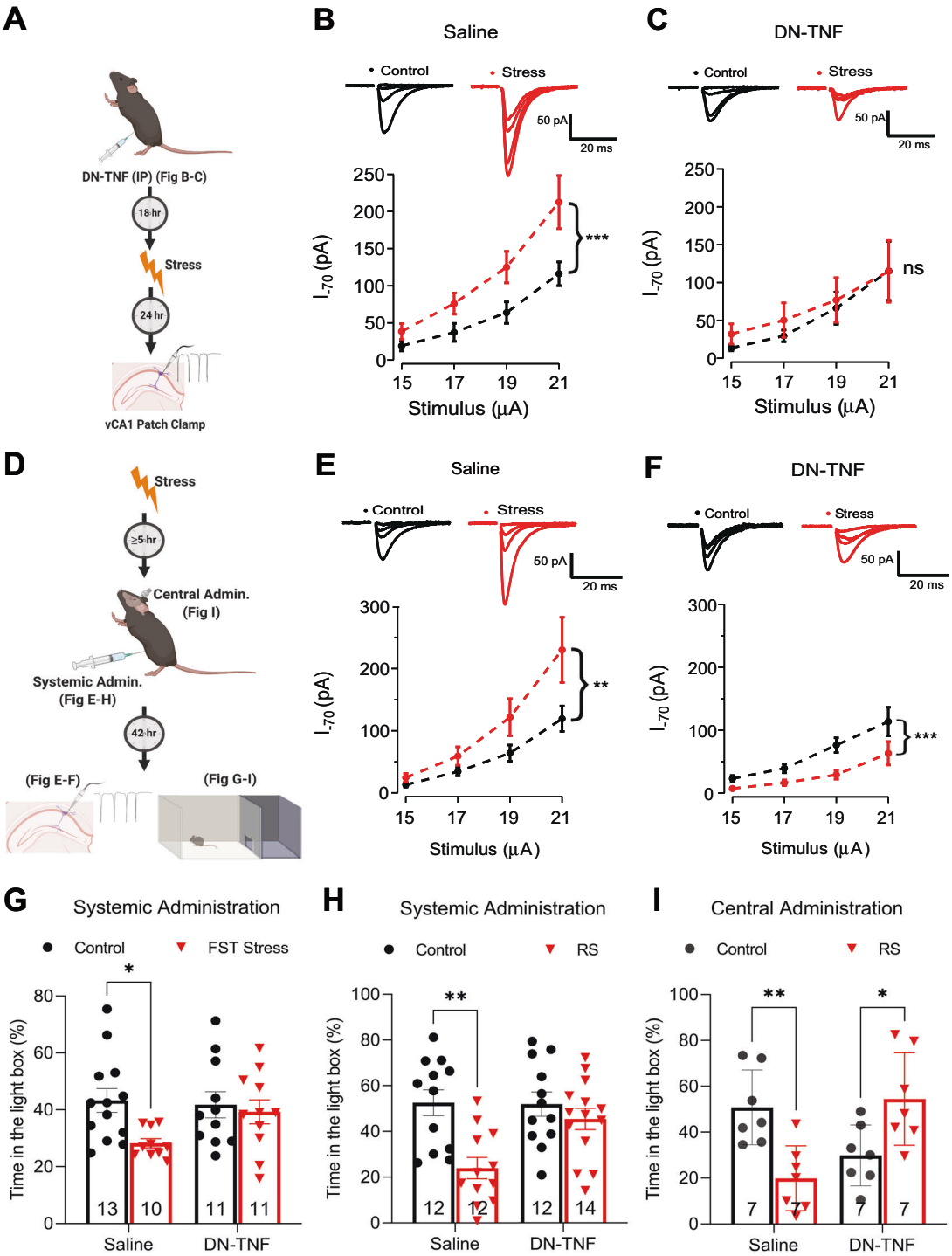

substantial potentiation of hippocampal synapses by Cort in vitro (Supplementary Fig. 7), other work suggests that this potentiation is not sustained beyond a few hours [57]. Further, slices from *TNF*$^{-/-}$ mice display an equal Cort-driven synaptic potentiation in vitro, but no sustained stress-induced hippocampal potentiation in vivo. Thus, we would argue that Cort is necessary to induce the stress response but the sustained synaptic potentiation in vivo is maintained by on-going TNF signaling.

Consistent with our findings, TNF can directly increase AMPAR content at CA1 hippocampal synapses [63] and increased output from the ventral hippocampus can drive anxiety-like behavior [32]. Thus, TNF is likely to drive the observed synaptic potentiation on CA1 pyramidal neurons, which may well be accompanied by decreased inhibition [64], and would result in increased activity of these cells. That blocking TNF signaling just within the ventral hippocampus is sufficient to prevent the stress-induced anxiety would argue that these synaptic changes in the ventral hippocampus are causative for the stress-induced increase in anxiety-like behavior.

Our data here also supports the idea that microglia are the source of the stress-induced elevation in TNF. Consistent with previous reports [15, 23, 46], we observe a stress-induced increase in markers of microglia activation, including increased Iba1 expression and altered microglia morphology. Moreover, we

Fig. 4 TNF antagonism post-stress reverses stress-induced plasticity and behavior. A. A schematic of the experiments performed in **B**, **C**. **B** Systemic (IP) administration of saline prior to stress does not interfere with stress-induced AMPAR current potentiation at vCA1-SC synapses (two-way ANOVA of the main effect of stress F (1, 58) = 14.5093, $p = 0.0003$; control: $n = 7$, $N = 5$, stress: $n = 10$, $N = 6$). **C**. Blocking TNF signaling through systemic (IP) administration of dominant negative TNF (DNTNF; 20 mg/kg) prior to stress blocks the observed potentiation (two-way ANOVA of the main effect of stress F (1, 44) = 0.4727, $p = 0.4954$; control: $n = 7$, $N = 3$, stress: $n = 6$, $N = 4$). **D** A schematic of the experiments performed in **E**–**I**. **E** Administering saline IP at 5 h post-stress does not block AMPAR mediated, vCA1-SC synaptic potentiation observed at 48 h post-stress (two-way ANOVA of the main effect of stress F (1, 84) = 6.5693, $p = 0.0122$; control: $n = 11$, $N = 7$, stress: $n = 12$, $N = 8$). **F** Systemic (IP) administration of DN-TNF 5 h after stress blocks the expression of stress-induced synaptic potentiation (two-way ANOVA of the main effect of stress F(1, 64) = 14.78, $p = 0.0003$; control: $n = 10$, $N = 5$, stress: $n = 8$, $N = 5$). **G**. Blocking TNF signaling via administering DN-TNF (IP; 20 mg/kg; 5 h post-stress) prevents anxiety-like behavior 48 h post-swim stress (two-way ANOVA of the main effect of stress F (1, 41) = 4.825, $p = 0.0338$; main effect of drug treatment F (1, 41) = 1.428, $p = 0.2390$; interaction of stress x drug treatment F (1, 41) = 2.470, $p = 0.1237$; Tukey's post hoc analyses of control saline versus FST saline $p = 0.0494$, control DN-TNF versus FST DN-TNF $p = 0.9714$). **H** TNF is similarly necessary for stress-induction of anxiety-like behavior following restraint stress (two-way ANOVA of the interaction of stress x drug treatment F (1, 46) = 4.692, $p = 0.0355$; Tukey's post hoc analyses of control saline versus RS saline $p = 0.0017$, control DN-TNF versus RS DN-TNF $p = 0.7908$). **I** Blocking TNF in the vHPC through local administration of DN-TNF (IC; 4.8 mg/kg; 5 h post-RS) prevents the development of anxiety-like behavior 48 h in response to stress (two-way ANOVA of the interaction of stress x drug treatment F (1, 24) = 20.58, $p = 0.0001$; Tukey's *post hoc* analyses of control saline versus RS saline $p = 0.0078$, of control DN-TNF versus RS DN-TNF $p = 0.0419$). $^{*}p < 0.05$, $^{**}p < 0.01$, $^{***}p < 0.001$. Data are presented as mean ± SEM. Sample sizes are indicated on the bar figure or in the caption.

observed an increase in TNF mRNA associated with microglia. The conditional deletion of TNF from microglia prevented the stress-induced increase in hippocampal TNF, and also prevented a stress-induced increase in anxiety-like behavior. However, we did observe a baseline shift in anxiety-like behavior in these mice, which was not seen in either the full TNF knockout or the astrocyte-specific knockout. This complicates the interpretation, and we have observed several changes in baseline behavior in the microglial-conditional mice (including increased aggression and fighting) that could drive other changes in baseline behavior. But despite the baseline shift, there should be adequate potential to express additional anxiety-like behavior as the mice are still spending over 20% of their time in the light compartment, and thus we do not believe that any floor effect is obscuring a stress-induced change in behavior. Importantly, when combined with the other data on stress-induced microglial activation and lack of TNF response to stress in the conditional mutant, we believe that a microglial source of stress-induced TNF is the most parsimonious hypothesis. Whether the microglial activation is due to Cort signaling is unclear at this point. Our data suggests that Cort signaling is critical for the stress-induced behavioral change, but direct activation will need to be tested. Microglia express both MR and GR [65, 66], and stress can act through GR to increase TNF levels [67, 68]. A glial target of Cort signaling would be consistent with the finding that conditional deletion of GR from forebrain excitatory neurons did not alter a stress-induced increase in anxiety-like behavior [69].

Other cytokines may also be released by activated microglia, and there is evidence that IL1 contributes to stress induced anxiety-like behavior [70], although the observed increase in IL1 was more transient than the increase in TNF. This could suggest that multiple cytokines are involved with the induction of the stress response but perhaps TNF has a unique role in maintaining the anxiety.

One interesting observation is the significant decrease in synaptic strength post-stress observed in $TNF^{-/-}$ and DN-TNF treated animals, which suggests that the synaptic strength is actually decreasing in response to stress. This might be indication of a countervailing resilience-type signal being unmasked in the absence of TNF signaling, though the nature of such a signal would need to be determined.

Critically, the functional consequences of this stress-induced potentiation can be reversed well after its onset by blocking TNF signaling. The synaptic potentiation is established within 2 h of the stressor, yet blocking TNF signaling 5 h afterwards is sufficient to reverse both the synaptic plasticity and the behavioral change. Thus, hippocampal TNF signaling is necessary for the maintenance of these changes. This may have therapeutic potential for cases in which the effects of stress are particularly detrimental as in post-traumatic stress disorder, where TNF-based therapeutics may hold potential to treat the chronic anxiety of such conditions.

REFERENCES

1. Brewin CR. Risk factor effect sizes in PTSD: what this means for intervention. J Trauma Dissociation. 2005;6:123–30. https://doi.org/10.1300/J229v06n02_11
2. McEwen BS, Bowles NP, Gray JD, Hill MN, Hunter RG, Karatsoreos IN, et al. Mechanisms of stress in the brain. Nat Neurosci. 2015;18:1353–63. https://doi.org/10.1038/nn.4086
3. Sorrells SF, Caso JR, Munhoz CD, Sapolsky RM. The stressed CNS: when glucocorticoids aggravate inflammation. Neuron. 2009;64:33–39. https://doi.org/10.1016/j.neuron.2009.09.032
4. Dhabhar FS. Enhancing versus suppressive effects of stress on immune function: implications for immunoprotection and immunopathology. Neuroimmunomodulation. 2009;16:300–17. https://doi.org/10.1159/000216188
5. Costa-Pinto FA, Palermo-Neto J. Neuroimmune interactions in stress. Neuroimmunomodulation. 2010;17:196–9. https://doi.org/10.1159/000258722
6. Tang Z, Ye G, Chen X, Pan M, Fu J, Fu T, et al. Peripheral proinflammatory cytokines in Chinese patients with generalised anxiety disorder. J Affect Disord. 2018;225:593–8. https://doi.org/10.1016/j.jad.2017.08.082
7. Hou R, Garner M, Holmes C, Osmond C, Teeling J, Lau L, et al. Peripheral inflammatory cytokines and immune balance in Generalised Anxiety Disorder: Case-controlled study. Brain Behav Immun. 2017;62:212–8. https://doi.org/10.1016/j.bbi.2017.01.021
8. Muscatell KA, Dedovic K, Slavich GM, Jarcho MR, Breen EC, Bower JE, et al. Greater amygdala activity and dorsomedial prefrontal-amygdala coupling are associated with enhanced inflammatory responses to stress. Brain Behav Immun. 2015;43:46–53. https://doi.org/10.1016/j.bbi.2014.06.201
9. Slavish DC, Graham-Engeland JE, Smyth JM, Engeland CG. Salivary markers of inflammation in response to acute stress. Brain Behav Immun. 2015;44:253–69. https://doi.org/10.1016/j.bbi.2014.08.008
10. You Z, Luo C, Zhang W, Chen Y, He J, Zhao Q, et al. Pro- and anti-inflammatory cytokines expression in rat's brain and spleen exposed to chronic mild stress: involvement in depression. Behav Brain Res. 2011;225:135–41. https://doi.org/10.1016/j.bbr.2011.07.006
11. Wohleb ES, Hanke ML, Corona AW, Powell ND, Stiner LM, Bailey MT, et al. beta-Adrenergic receptor antagonism prevents anxiety-like behavior and microglial reactivity induced by repeated social defeat. J Neurosci. 2011;31:6277–88. https://doi.org/10.1523/JNEUROSCI.0450-11.2011
12. Caso JR, Lizasoain I, Lorenzo P, Moro MA, Leza JC. The role of tumor necrosis factor-alpha in stress-induced worsening of cerebral ischemia in rats. Neuroscience. 2006;142:59–69. https://doi.org/10.1016/j.neuroscience.2006.06.009
13. Turnbull AV, Rivier CL. Regulation of the hypothalamic-pituitary-adrenal axis by cytokines: actions and mechanisms of action. Physiol Rev. 1999;79:1–71.
14. Qing H, Desrouleaux R, Israni-Winger K, Mineur YS, Fogelman N, Zhang C, et al. Origin and function of stress-induced IL-6 in murine models. Cell. 2020;182:372–87. https://doi.org/10.1016/j.cell.2020.05.054. e314
15. Serrats J, Grigoleit JS, Alvarez-Salas E, Sawchenko PE. Pro-inflammatory immune-to-brain signaling is involved in neuroendocrine responses to acute emotional stress. Brain. Behav. Immun. 2017;62:53–63. https://doi.org/10.1016/j.bbi.2017.02.003
16. Koo JW, Duman RS. IL-1beta is an essential mediator of the antineurogenic and anhedonic effects of stress. Proc Natl Acad Sci USA. 2008;105:751–6. https://doi.org/10.1073/pnas.0708092105

17. Iwata M, Ota KT, Li XY, Sakaue F, Li N, Dutheil S, et al. Psychological stress activates the inflammasome via release of adenosine triphosphate and stimulation of the purinergic type 2X7 receptor. Biol Psychiatry. 2016;80:12–22. https://doi.org/10.1016/j.biopsych.2015.11.026
18. Camara ML, Corrigan F, Jaehne EJ, Jawahar MC, Anscomb H, Baune BT. Effects of centrally administered etanercept on behavior, microglia, and astrocytes in mice following a peripheral immune challenge. Neuropsychopharmacol: Off Publ Am Coll Neuropsychopharmacol. 2015;40:502–12. https://doi.org/10.1038/npp.2014.199
19. Chen J, Song Y, Yang J, Zhang Y, Zhao P, Zhu XJ, et al. The contribution of TNF-alpha in the amygdala to anxiety in mice with persistent inflammatory pain. Neurosci Lett. 2013;541:275–80. https://doi.org/10.1016/j.neulet.2013.02.005
20. Fourrier C, Bosch-Bouju C, Boursereau R, Sauvant J, Aubert A, Capuron L, et al. Brain tumor necrosis factor-alpha mediates anxiety-like behavior in a mouse model of severe obesity. Brain Behav Immun. 2019;77:25–36. https://doi.org/10.1016/j.bbi.2018.11.316
21. Haji N, Mandolesi G, Gentile A, Sacchetti L, Fresegna D, Rossi S, et al. TNF-alpha-mediated anxiety in a mouse model of multiple sclerosis. Exp Neurol. 2012;237:296–303. https://doi.org/10.1016/j.expneurol.2012.07.010
22. O'Connor KA, Johnson JD, Hansen MK, Wieseler Frank JL, Maksimova E, Watkins LR, et al. Peripheral and central proinflammatory cytokine response to a severe acute stressor. Brain Res. 2003;991:123–32.
23. Ohgidani M, Kato TA, Sagata N, Hayakawa K, Shimokawa N, Sato-Kasai M, et al. TNF-alpha from hippocampal microglia induces working memory deficits by acute stress in mice. Brain Behav Immun. 2016;55:17–24. https://doi.org/10.1016/j.bbi.2015.08.022
24. Vecchiarelli HA, Gandhi CP, Gray JM, Morena M, Hassan KI, Hill MN. Divergent responses of inflammatory mediators within the amygdala and medial prefrontal cortex to acute psychological stress. Brain Behav Immun. 2016;51:70–91. https://doi.org/10.1016/j.bbi.2015.07.026
25. Madrigal JL, Hurtado O, Moro MA, Lizasoain I, Lorenzo P, Castrillo A, et al. The increase in TNF-alpha levels is implicated in NF-kappaB activation and inducible nitric oxide synthase expression in brain cortex after immobilization stress. Neuropsychopharmacol: Off Publ Am Coll Neuropsychopharmacol. 2002;26:155–63. https://doi.org/10.1016/S0893-133X(01)00292-5
26. Nguyen KT, Deak T, Owens SM, Kohno T, Fleshner M, Watkins LR, et al. Exposure to acute stress induces brain interleukin-1beta protein in the rat. J Neurosci. 1998;18:2239–46.
27. Goshen I, Kreisel T, Ben-Menachem-Zidon O, Licht T, Weidenfeld J, Ben-Hur T, et al. Brain interleukin-1 mediates chronic stress-induced depression in mice via adrenocortical activation and hippocampal neurogenesis suppression. Mol Psychiatry. 2008;13:717–28. https://doi.org/10.1038/sj.mp.4002055
28. Fanselow MS, Dong HW. Are the dorsal and ventral hippocampus functionally distinct structures? Neuron. 2010;65:7–19. https://doi.org/10.1016/j.neuron.2009.11.031
29. Strange BA, Witter MP, Lein ES, Moser EI. Functional organization of the hippocampal longitudinal axis. Nat Rev Neurosci. 2014;15:655–69. https://doi.org/10.1038/nrn3785
30. Bannerman DM, Deacon RMJ, Offen S, Friswell J, Grubb M, Rawlins JNP. Double dissociation of function within the hippocampus: spatial memory and hyponeophagia. Behav Neurosci. 2002;116:884–901.
31. Kjelstrup KG, Tuvnes FA, Steffenach HA, Murison R, Moser EI, Moser MB. Reduced fear expression after lesions of the ventral hippocampus. Proc Natl Acad Sci USA. 2002;99:10825–30. https://doi.org/10.1073/pnas.152112399
32. Jimenez JC, Su K, Goldberg AR, Luna VM, Biane JS, Ordek G, et al. Anxiety cells in a Hippocampal-Hypothalamic circuit. Neuron. 2018;97:670–83. e676 https://doi.org/10.1016/j.neuron.2018.01.016
33. Felix-Ortiz AC, Beyeler A, Seo C, Leppla CA, Wildes CP, Tye KM. BLA to vHPC inputs modulate anxiety-related behaviors. Neuron. 2013;79:658–64. https://doi.org/10.1016/j.neuron.2013.06.016
34. Kheirbek MA, Drew LJ, Burghardt NS, Costantini DO, Tannenholz L, Ahmari SE, et al. Differential control of learning and anxiety along the dorsoventral axis of the dentate gyrus. Neuron. 2013;77:955–68. https://doi.org/10.1016/j.neuron.2012.12.038
35. Kjaerby C, Athilingam J, Robinson SE, Iafrati J, Sohal VS. Serotonin 1B receptors regulate prefrontal function by gating callosal and hippocampal inputs. Cell Rep. 2016;17:2882–90. https://doi.org/10.1016/j.celrep.2016.11.036
36. Wu MV, Hen R. Functional dissociation of adult-born neurons along the dorsoventral axis of the dentate gyrus. Hippocampus. 2014;24:751–61. https://doi.org/10.1002/hipo.22265
37. Parfitt GM, Nguyen R, Bang JY, Aqrabawi AJ, Tran MM, Seo DK, et al. Bidirectional control of anxiety-related behaviors in mice: role of inputs arising from the ventral hippocampus to the lateral septum and medial prefrontal cortex. Neuropsychopharmacol: Off Publ Am Coll Neuropsychopharmacol. 2017;42:1715–28. https://doi.org/10.1038/npp.2017.56
38. Padilla-Coreano N, Bolkan SS, Pierce GM, Blackman DR, Hardin WD, Garcia-Garcia AL, et al. Direct ventral hippocampal-prefrontal input is required for anxiety-related neural activity and behavior. Neuron. 2016;89:857–66. https://doi.org/10.1016/j.neuron.2016.01.011
39. Radley JJ, Sawchenko PE. A common substrate for prefrontal and hippocampal inhibition of the neuroendocrine stress response. J Neurosci. 2011;31:9683–95. https://doi.org/10.1523/JNEUROSCI.6040-10.2011
40. Stellwagen D, Malenka RC. Synaptic scaling mediated by glial TNF-alpha. Nature. 2006;440:1054–9.
41. Peschon JJ, Torrance DS, Stocking KL, Glaccum MB, Otten C, Willis CR, et al. TNF receptor-deficient mice reveal divergent roles for p55 and p75 in several models of inflammation. J Immunol. 1998;160:943–52.
42. Grivennikov SI, Tumanov AV, Liepinsh DJ, Kruglov AA, Marakusha BI, Shakhov AN, et al. Distinct and nonredundant in vivo functions of TNF produced by t cells and macrophages/neutrophils: protective and deleterious effects. Immunity. 2005;22:93–104. https://doi.org/10.1016/j.immuni.2004.11.016
43. Bajenaru ML, Zhu Y, Hedrick M, Donahoe J, Parada LF, Gutmann DH. Astrocyte-specific inactivation of the neurofibromatosis 1 gene (NF1) is insufficient for astrocytoma formation. Mol Cell Biol. 2002;22:5100–13. https://doi.org/10.1128/mcb.22.14.5100-5113.2002
44. Yona S, Kim KW, Wolf Y, Mildner A, Varol D, Breker M, et al. Fate mapping reveals origins and dynamics of monocytes and tissue macrophages under homeostasis. Immunity. 2013;38:79–91. https://doi.org/10.1016/j.immuni.2012.12.001
45. Cullinan WE, Herman JP, Battaglia DF, Akil H, Watson SJ. Pattern and time course of immediate early gene expression in rat brain following acute stress. Neuroscience. 1995;64:477–505. https://doi.org/10.1016/0306-4522(94)00355-9
46. Calcia MA, Bonsall DR, Bloomfield PS, Selvaraj S, Barichello T, Howes OD. Stress and neuroinflammation: a systematic review of the effects of stress on microglia and the implications for mental illness. Psychopharmacology. 2016;233:1637–50. https://doi.org/10.1007/s00213-016-4218-9
47. Yuen EY, Liu W, Karatsoreos IN, Feng J, McEwen BS, Yan Z. Acute stress enhances glutamatergic transmission in prefrontal cortex and facilitates working memory. Proc Natl Acad Sci USA. 2009;106:14075–9. https://doi.org/10.1073/pnas.0906791106
48. Yuen EY, Liu W, Karatsoreos IN, Ren Y, Feng J, McEwen BS, et al. Mechanisms for acute stress-induced enhancement of glutamatergic transmission and working memory. Mol Psychiatry. 2011;16:156–70. https://doi.org/10.1038/mp.2010.50
49. Campioni MR, Xu M, McGehee DS. Stress-induced changes in nucleus accumbens glutamate synaptic plasticity. J Neurophysiol. 2009;101:3192–8. https://doi.org/10.1152/jn.91111.2008
50. Saal D, Dong Y, Bonci A, Malenka RC. Drugs of abuse and stress trigger a common synaptic adaptation in dopamine neurons. Neuron. 2003;37:577–82.
51. Kuzmiski JB, Marty V, Baimoukhametova DV, Bains JS. Stress-induced priming of glutamate synapses unmasks associative short-term plasticity. Nat Neurosci. 2010;13:1257–64. https://doi.org/10.1038/nn.2629
52. Musazzi L, Milanese M, Farisello P, Zappettini S, Tardito D, Barbiero VS, et al. Acute stress increases depolarization-evoked glutamate release in the rat prefrontal/frontal cortex: the dampening action of antidepressants. PloS One. 2010;5:e8566 https://doi.org/10.1371/journal.pone.0008566
53. Treccani G, Musazzi L, Perego C, Milanese M, Nava N, Bonifacino T, et al. Stress and corticosterone increase the readily releasable pool of glutamate vesicles in synaptic terminals of prefrontal and frontal cortex. Mol Psychiatry. 2014;19:433–43. https://doi.org/10.1038/mp.2014.5
54. Gray JD, Rubin TG, Hunter RG, McEwen BS. Hippocampal gene expression changes underlying stress sensitization and recovery. Mol Psychiatry. 2014;19:1171–8. https://doi.org/10.1038/mp.2013.175
55. Morsink MC, Van Gemert NG, Steenbergen PJ, Joels M, De Kloet ER, Datson NA. Rapid glucocorticoid effects on the expression of hippocampal neurotransmission-related genes. Brain Res. 2007;1150:14–20. https://doi.org/10.1016/j.brainres.2007.02.083
56. Joels M, Velzing E, Nair S, Verkuyl JM, Karst H. Acute stress increases calcium current amplitude in rat hippocampus: temporal changes in physiology and gene expression. Eur J Neurosci. 2003;18:1315–24.
57. Karst H, Joels M. Corticosterone slowly enhances miniature excitatory post-synaptic current amplitude in mice CA1 hippocampal cells. J Neurophysiol. 2005;94:3479–86. https://doi.org/10.1152/jn.00143.2005
58. Groc L, Choquet D, Chaouloff F. The stress hormone corticosterone conditions AMPAR surface trafficking and synaptic potentiation. Nat Neurosci. 2008;11:868–70. https://doi.org/10.1038/nn.2150
59. Steed PM, Tansey G, Zalevsky J, Zhukovsky EA, Desjarlais JR, Szymkowski DE, et al. Inactivation of TNF signaling by rationally designed dominant-negative TNF variants. Science. 2003;301:1895–8.
60. Lewitus GM, Konefal SC, Greenhalgh AD, Pribiag H, Augereau K, Stellwagen D. Microglial TNF-alpha suppresses cocaine-induced plasticity and behavioral sensitization. Neuron. 2016;90:483–91. https://doi.org/10.1016/j.neuron.2016.03.030
61. Lewitus GM, Pribiag H, Duseja R, St-Hilaire M, Stellwagen D. An adaptive role of TNFalpha in the regulation of striatal synapses. J Neurosci. 2014;34:6146–55. https://doi.org/10.1523/JNEUROSCI.3481-13.2014

62. Popoli M, Yan Z, McEwen BS, Sanacora G. The stressed synapse: the impact of stress and glucocorticoids on glutamate transmission. Nat Rev Neurosci. 2011;13:22–37. https://doi.org/10.1038/nrn3138
63. Beattie EC, Stellwagen D, Morishita W, Bresnahan JC, Ha BK, Von Zastrow M, et al. Control of synaptic strength by glial TNFalpha. Science. 2002;295:2282–5.
64. Stellwagen D, Beattie EC, Seo JY, Malenka RC. Differential regulation of AMPA receptor and GABA receptor trafficking by tumor necrosis factor-alpha. J Neurosci. 2005;25:3219–28.
65. Brocca ME, Pietranera L, de Kloet ER, De Nicola AF. Mineralocorticoid receptors, neuroinflammation and hypertensive encephalopathy. Cell Mol Neurobiol. 2019;39:483–92. https://doi.org/10.1007/s10571-018-0610-9
66. Chantong B, Kratschmar DV, Nashev LG, Balazs Z, Odermatt A. Mineralocorticoid and glucocorticoid receptors differentially regulate NF-kappaB activity and pro-inflammatory cytokine production in murine BV-2 microglial cells. J Neuroinflammation. 2012;9:260 https://doi.org/10.1186/1742-2094-9-260
67. Frank MG, Thompson BM, Watkins LR, Maier SF. Glucocorticoids mediate stress-induced priming of microglial pro-inflammatory responses. Brain Behav Immun. 2012;26:337–45. https://doi.org/10.1016/j.bbi.2011.10.005
68. Wang N, Ma H, Li Z, Gao Y, Cao X, Jiang Y, et al. Chronic unpredictable stress exacerbates surgery-induced sickness behavior and neuroinflammatory responses via glucocorticoids secretion in adult rats. PloS One. 2017;12:e0183077 https://doi.org/10.1371/journal.pone.0183077
69. Furay AR, Bruestle AE, Herman JP. The role of the forebrain glucocorticoid receptor in acute and chronic stress. Endocrinology. 2008;149:5482–90. https://doi.org/10.1210/en.2008-0642
70. McKim DB, Weber MD, Niraula A, Sawicki CM, Liu X, Jarrett BL, et al. Microglial recruitment of IL-1beta-producing monocytes to brain endothelium causes stress-induced anxiety. Mol Psychiatry. 2018;23:1421–31. https://doi.org/10.1038/mp.2017.64

ACKNOWLEDGEMENTS

This work was supported by the Canadian Institutes for Health Research and Natural Sciences and Engineering Research Council of Canada. G.M.K. was supported by a fellowship from the Canada First Research Excellence Fund, awarded to McGill University for the Healthy Brains for Healthy Lives initiative. H.F.A. was supported by doctoral awards from the Heart and Stroke Foundation of Canada, and the Research Institute of the McGill University Health Centre. We kindly thank Xencor for the donation of XPro1595. Schematic figures were created using BioRender.

AUTHOR CONTRIBUTIONS

G.M.K, H.F.A., and D.S. designed the research; G.M.K, H.F.A., Y.N., R.H., and A.K. performed experiments; G.M.K, H.F.A., Y.N., and R.H. analyzed data; G.M.K, H.F.A., and D.S. wrote the manuscript.

COMPETING INTERESTS

The authors declare no competing interests.

ADDITIONAL INFORMATION

Supplementary information The online version contains supplementary material available at https://doi.org/10.1038/s41380-022-01737-x.

Correspondence and requests for materials should be addressed to David Stellwagen.

Reprints and permission information is available at http://www.nature.com/reprints

Publisher's note Springer Nature remains neutral with regard to jurisdictional claims in published maps and institutional affiliations.